Available online at www.sciencedirect.com
SCIENCE DIRECT®
Acta Materialia 53 (2005) 1611–1619
Acta MATERIALIA
www.actamat-journals.com

Excess free volume in metallic glasses measured by X-ray diffraction

Alain Reza Yavari [a,*], Alain Le Moulec [a], Akihisa Inoue [b], Nobuyuki Nishiyama [b], Nicoleta Lupu [a,b], Eiichiro Matsubara [b], Walter José Botta [a,1], Gavin Vaughan [c], Marco Di Michiel [c], Åke Kvick [c]

[a] *Euronano, LTPCM-CNRS, Institut National Polytechnique de Grenoble, 1130 rue de la Piscine, BP 75, 38402 St-Martin-d'Hères Campus, France*
[b] *Institute for Materials Research, Tohoku University, 980-8577 Sendai, Japan*
[c] *European Synchrotron Radiation Facilities (ESRF), 38042 Grenoble, France*

Received 6 August 2004; received in revised form 2 December 2004; accepted 7 December 2004
Available online 13 January 2005

Abstract

In crystalline materials, lattice expansion as measured by diffraction methods differs from the expansion of the sample dimensions as measured by dilatometry, due to the contribution of thermal vacancies to the latter. We have found that in glassy materials and metallic glasses in particular, this is not the case for the contribution of free volume. These findings are the first direct experimental confirmation of simulation results indicating that atomic size holes are unstable in glasses such that free volume is dispersed randomly. This allows direct measurement of excess free volume in glasses using diffraction methods in place of dilatometry, which is difficult to use once the sample softens at the glass transition temperature T_g and above. Quenched-in and deformation-induced free-volume ΔV_f were measured by X-ray diffraction in transmission during heating using synchrotron light. The measured thermal expansion coefficients α_{th} were the same as in dilatometry. The glass transition T_g appeared as a break in the value of α_{th} at T_g. The "change-of-slope method" was applied to the kinetics of relaxation to derive the activation energy for the free-volume annihilation process.
© 2004 Acta Materialia Inc. Published by Elsevier Ltd. All rights reserved.

Keywords: Metallic glass; Free volume; Deformation; Synchrotron light; Diffraction; Thermal expansion; Relaxation

1. Introduction

In 1959, Cohen and Turnbull [1], using a "free-volume" formulation of the viscosity, predicted that a metallic glass could be obtained if the melt were quenched fast enough to bypass crystal nucleation and growth. The first metallic glasses were obtained by Duwez and co-workers in 1960 [2] using splat-quenching of droplets of near eutectic metal-metalloid liquid alloys such as Au–Si. In the two decades that followed this initial discovery, a large number of binary and multicomponent metal–metal and metal-metalloid alloys were obtained in the glassy state by rapid solidification of the liquid using a technique referred to as "melt-spinning" which at cooling rates of the order of 10^5 K/s produces glassy foils or ribbons with thicknesses of tens of micrometers.

The rationale guiding these efforts was to use alloying to expand the stability of the liquid state down to lower temperatures as in eutectic compositions and to slow down the atomic diffusion processes controlling the nucleation and growth of crystalline phases [3]

* Corresponding author. Tel.: +33 476 826 641; fax: +33 476 826 516.
E-mail addresses: yavari@ltpcm.inpg.fr, euronano@ltpcm.inpg.fr (A.R. Yavari).
[1] Permanent address. Universidade Federal de São Carlos, DEMa, CP 676, 13.565-905 São Carlos, SP, Brazil.

1359-6454/$30.00 © 2004 Acta Materialia Inc. Published by Elsevier Ltd. All rights reserved.
doi:10.1016/j.actamat.2004.12.011

by increasing the viscosity of the undercooled liquid. Since 1990, these efforts have lead to the development of a large number of complex alloys that can be cooled into bulk glass form up to several centimeters thick [4–7] at cooling rates less than 1–100 K/s by conventional methods such as copper-mold casting. Some recently discovered metallic glasses exhibit record mechanical and magnetic properties as recently reported by the authors [8]. As for the more conventional SiO_2-based oxide glass formers such as window glass and pyrex, the kinetics of diffusive atomic motion in metallic undercooled melts can be modeled using a dispersion of "holes" or "free volume" in the liquid in much the same way as "vacancies" or empty lattice sites control diffusive jumps of atoms in a crystal [9–11].

The viscosity η of the undercooled liquid can then be written as

$$\eta \sim \eta_0 e^{\delta V_a/V_f} = \eta_0 e^{\delta V_a/V_0 \alpha_{th}(T-T_0)}, \quad (1)$$

where η_0 is a materials-specific pre-exponential, V_f is the free volume, V_a is the mean atomic volume, δ is an adjustable parameter, V_0 is V_a at a reference temperature T_0 and α_{th} is the volume coefficient of thermal expansion. Through the Stokes–Einstein relation, free-volume can be shown to control atomic diffusion much like vacancies do in crystal lattices.

Below a glass transition temperature T_g, the free-volume V_f content becomes negligible, the viscosity diverges to values far above 10^{12} Poise and the atoms freeze into a glassy state. In the absence of free volume, the relaxed glassy state is then kinetically stable below T_g. However, as the quench rate is increased, some of the liquid's free volume is trapped into the glassy state. Over the years, various techniques (most directly by dilatometry) have demonstrated annihilation of quenched-in free volume during thermal annealing of rapidly quenched metallic glasses with mass density increases of less than 0.5% [4,12]. However, the use of most dilatometric devices for V_f measurements becomes inaccurate once the sample softens at the glass transition temperature T_g and above. We have previously reported the first measurements of the glass transition T_g in metallic glasses using diffraction methods [13,14]. Here we report measurements of quenched-in and deformation-induced free-volume ΔV_f in glassy $Pd_{40}Cu_{30}Ni_{10}P_{20}$ and other glasses by in situ X-ray diffraction in transmission during heating cycles. We find that ΔV_f anneals out during heating up to T_g, at which temperature all thermo-mechanical history was erased. The measured thermal expansion coefficients α_{th} were found to be the same as in dilatometry and glass transitions T_g appeared clearly as a break in the value of α_{th} as the glass transforms to a supercooled liquid state during heating.

2. Experimental method

Diffraction spectra, obtained in transmission with a high-intensity high-energy monochromatic beam, were used to continuously follow the evolution of the glassy alloys during heating from the glassy state across T_g to the superheated liquid state. Ribbon samples about 30 μm thick were melt-spun on a copper wheel under argon gas. Heavily deformed continuous foil packs with individual foil thickness of 1–3 μm were obtained by low amplitude milling of the melt-spun ribbons in a vibratory mill with a single 6 cm diameter ball under argon gas. The glassy alloy ribbons and foil packs were cut into 3 cm long pieces with thickness and width less than 1 mm to enter capillary tubes sealed under argon gas and placed on a computer-controlled Linkam hot stage. The white radiation on the ID11 beam line of the European Synchrotron Radiation Facilities (ESRF) was monochromatized using a nitrogen-cooled double crystal silicon monochromater. The photon energy was 90 keV corresponding to an X-ray wave-length of about 0.0137 nm. The heating and cooling rate was 10 K/min. Diffracted intensity in transmission through the capillary in the hot stage was recorded by a 2-dimensional CCD camera placed perpendicular to the incident beam away from the specimen. Acquisition and data processing times were such that a full spectrum was obtained about every 3 s. Further information can be found in previous publications [15,16]. X-ray measurements were carried out in the wave-vector range, Q from 0 to 14.5 A^{-1}. The intensity data below $Q = 0.7$ A^{-1} were smoothly extrapolated to zero. The polarization effect was zero due to the geometry used in the synchrotron setup. The effect of absorption was estimated to be of the order of 0.7–2.5%. Since the accuracy in $I(Q)$ determination was of the same magnitude, the absorption correction was neglected in the present study. Compton scattering was corrected using the values provided by Cromer and Mann [17] and the so-called Breit recoil factor. The generalized Krogh–Moe–Norman method [18] with the atomic scattering factors tabulated in [19] and including the anomalous dispersion corrections [20] were used to normalize the intensity data.

The reduced radial distribution function,

$$G(r) = 4\pi r[\rho(r) - \rho_0] = \frac{2}{\pi}\int_0^\infty Q \cdot I(Q)\sin(Qr)\,dQ, \quad (2)$$

was estimated from $Q \cdot I(Q)$ by the usual Fourier transformation, where $\rho(r)$ is the radial density function and ρ_0 is the average atomic number density. The pair distribution function $g(r)$ was then derived using:

$$g(r) = \frac{\rho(r)}{\rho_0} = 1 + \frac{G(r)}{4\pi r \rho_0}. \quad (3)$$

3. Results

The experimental setup for in situ diffraction in transmission yields diffraction patterns such as shown in the picture of Fig. 1 every few seconds. The intensity patterns are concentric rings much as in transmission electron microscopy. Radial integration of the rings yields the intensity $I(Q)$ versus wave-vector Q curves.

The samples are then heated and cooled at will and yield intensity $I(Q)$ versus wave vector Q curves for the desired temperatures as shown in the example of Fig. 2.

The pair distribution functions $g(r)$ (Fig. 3) are then derived from $Q \cdot I(Q)$ by the usual Fourier transformations Eqs. (2) and (3).

While very small changes can be observed during structural relaxation if Fig. 3(b) is blown up, the most important feature of the pair distribution functions

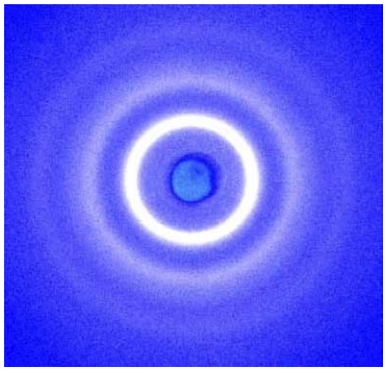

Fig. 1. Typical in situ diffraction data of a glass obtained in transmission in the form of concentric rings much as in transmission electron microscopy. Radial integration of the rings yields the intensity $I(Q)$ versus wave-vector Q curves.

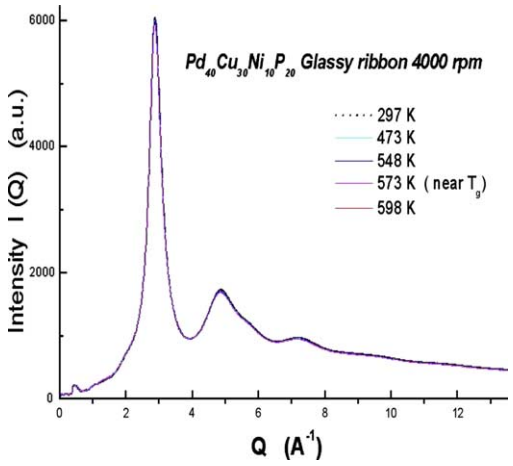

Fig. 2. Intensity $I(Q)$ versus wave-vector Q at temperatures below and above the glass transition T_g for glassy $Pd_{40}Cu_{30}Ni_{10}P_{20}$.

PDFs is their similarity regardless of the temperature (not fully relaxed below T_g and fully relaxed at or above T_g).

Previous (ex situ) diffraction studies of the effect of annealing on the PDFs of simpler (binary) metallic glasses of both metal-metalloid type [21] and metal–metal type [22] also showed small changes with for example increases of about 2% of the area for the roughly 11 nearest neighbors of the 1st nearest-neighbor peak. The present bulk glass forming alloys are more complex and more densely packed [23] and more recent in situ diffraction studies showed little change in the structure factor of bulk glass forming alloys across the glass transition [24]. The above results confirm that the packing structure of bulk metallic glasses (topological and chemical short and medium range order) is nearly the same above T_g in supercooled liquid state and below T_g in the glassy state and that as predicted and modeled

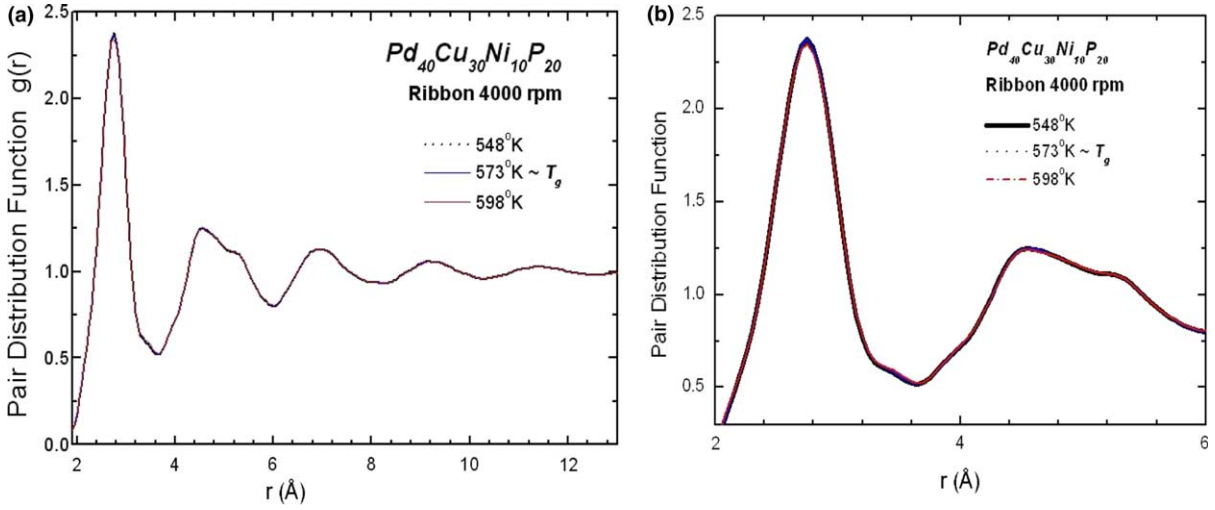

Fig. 3. (a) Pair distribution functions (PDF) derived from in situ diffraction at temperatures below and above the glass transition T_g for glassy $Pd_{40}Cu_{30}Ni_{10}P_{20}$. (b) Details of PDF for first two nearest neighbour shells below and above the glass transition T_g for glassy $Pd_{40}Cu_{30}Ni_{10}P_{20}$.

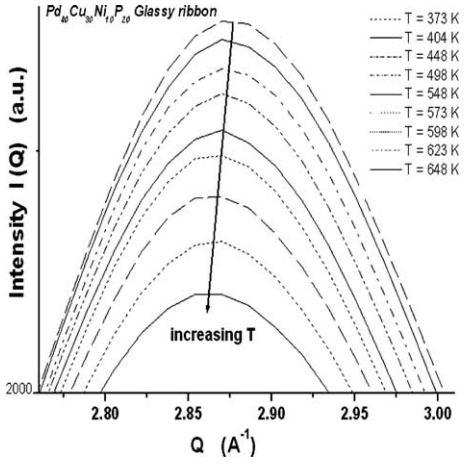

Fig. 4. Variation of Q_{max}, the position of the maximum diffracted intensity $I(Q)$ with temperature as a result of thermal expansion. Any deviation from reversibility would be due to relaxation.

previously [25,26] the free volume content is what distinguishes the glassy and the supercooled liquid states. However, PDFs cannot be used to derive volume or density variation as the density ρ_0 is an input for PDF derivation (see Eqs. (2) and (3)). As already mentioned, densification during structural relaxation has been measured to be less than 0.5% by for example Chen [4] using dilatometry and the authors [23] using density measurements before and after annealing.

In view of the above results and discussion, we decided as the next step, to treat the glassy state as a rigid isotropic solid up to T_g. In this approach, the successive broad maxima of the diffraction patterns will elastically move to lower Q values with increasing temperature (Fig. 4) as a result of thermal expansion and reversibly return to their initial Q_0 position upon cooling. Any deviation from this reversibility would then be discussed in terms of structural relaxation.

In order to search for irreversible phenomena, we follow Ehrenfest as described in [27,28]. The Ehrenfest relation is obtainable from the Debye formula for the scattering intensity $I(Q)$ and the square of the structure factor $F(Q)^2$ which is proportional to $(\sin Q.a/Q.a)$ for average interatomic separation "a". Setting the derivative of $(\sin Q.a)/Q.a$ with respect to "$Q.a$" equal to zero, one finds that it goes through a succession of maxima with the first and the most important occurring at $Q_{max} = 4\pi \sin\theta_m/\lambda = 1.23(2\pi/a)$ which is called the Ehrenfest relation [27] and which yields a characteristic dimension "a". The consequence would be that the variation with temperature of wave-vector Q_{max} of the first diffracted intensity $I(Q_{max})$ maximum will be inversely proportional to the mean atomic spacing. Thus it follows that the third power of Q_{max} will scale with the coefficient of volume thermal expansion of glassy structure as in:

$$\left\{\frac{Q_{max}(T^0)}{Q_{max}(T)}\right\}^3 = \left\{\frac{V(T)}{V(T^0)}\right\} = \{1 + \alpha_{th}(T - T^0)\}, \qquad (4)$$

where α_{th} is the volume coefficient of thermal expansion below T_g as long as no structural change occurs and corresponds to the temperature slope or derivative of the reduced mean atomic volume $\{V(T)/V(T^0)\}$ at T, with the reference T^0 corresponding to room temperature. From theory the proportionality constant relating Q_{max} (T) to $(1/a)$ and $V(T)$ in Eq. (4) can change if the structure of the glass and in particular the chemical order or the nature of the bonding changes significantly. Therefore, how precisely changes in Q_{max} can allow measurement of changes in free volume content during relaxation annealing has not yet been established but will be tested in what follows.

3.1. Excess free-volume ΔV_f in metallic glasses, effect of quenching and deformation

Fig. 5 shows plots of Eq. (4) for rapidly solidified glassy $Pd_{40}Cu_{30}Ni_{10}P_{20}$ ribbon during thermal cycling at 10 K/min. This composition is of the best easy glass former family and the glassy state can be maintained during cyclic heating and cooling to well above T_g [29].

It is seen that during initial heating the slope is constant with α_{th} about 5×10^{-5} K^{-1} or a linear coefficient of thermal expansion of 1.66×10^{-5} K^{-1} which is exactly the value measured by dilatometry [29]. From about $T = 425$ K the plot dips until reaching

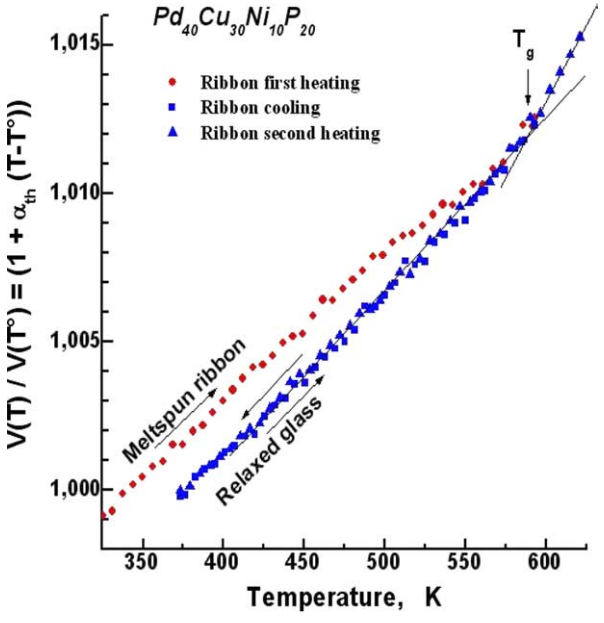

Fig. 5. Reduced volume per atom of Eq. (2) for rapidly quenched glass showing relaxation from 425 K up to $T_g = 590$ K.

Edited by Foxit Reader
Copyright(C) by Foxit Software Company,2005-2008
For Evaluation Only.

$T_g = 590$ K as determined by calorimetry (Fig. 6). A similar behaviour is observed in Pd-based glasses by dilatometry [4] when the apparatus is of the type that minimizes stress to the specimen (Fig. 7). Subsequent heating and cooling shows only reversible dilatation and contraction with the same slope as the initial one indicating that the quenched state of the glass has densified to a fully relaxed state during heating to T_g. As expected, a slope change occurs at T_g as the glass goes over to the supercooled liquid state. The volume difference between the initial as-quenched state (start of the first heating) and the subsequent relaxed state observed during T-cycling after heating to $T > T_g$ is about 0.2% which corresponds well to densification of other melt-spun metallic glasses as measured by dilatometry [4] or creep measurements [30] and as discussed in terms of the free-volume interpretation of the glass-transition [25].

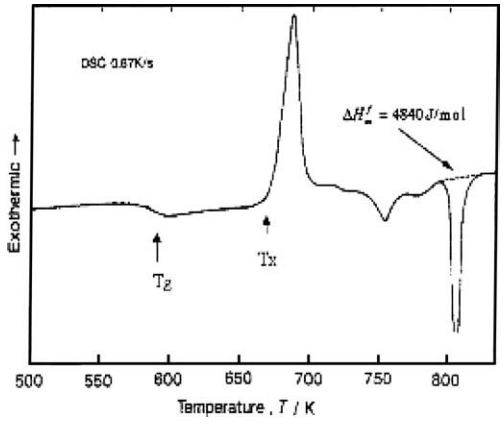

Fig. 6. Differential thermal analysis (DSC) of the glass of Fig. 4 showing glass transition at $T_g = 590$ K.

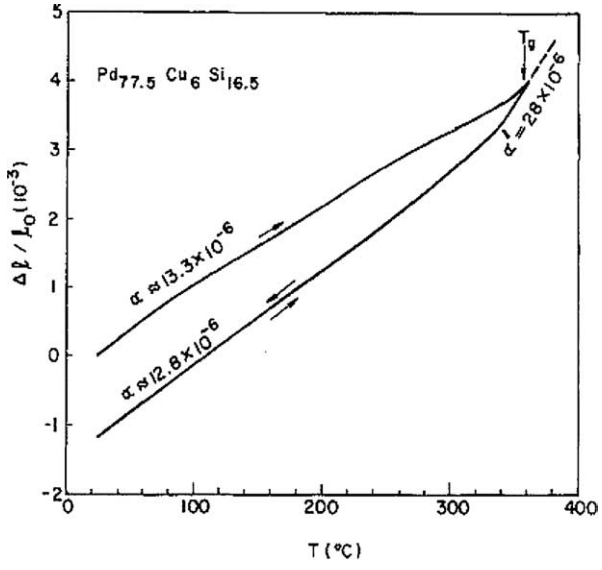

Fig. 7. Length change (dilatation) of a glassy Pd-based melt-spun ribbon showing densification towards the relaxed glassy state attained near T_g. A change of slope and the thermal expansion at T_g is clearly visible [4].

Fig. 8 shows the results of a similar in situ heating cycle experiment on the same glassy $Pd_{40}Cu_{30}Ni_{10}P_{20}$ ribbon but after severe plastic deformation to reduce ribbon thickness. Ribbon thicknesses are reduced from about 30 μm to about 1–3 μm corresponding to a thickness reduction of 90–97% by "gentle" milling using a single-ball vibrating mill as seen in the scanning electron microscope SEM image of the ribbon stacks (Fig. 9).

For comparison, the results of the previous Fig. 5 for the as-quenched (un-deformed) ribbon are also included in Fig. 8.

This comparison highlights several interesting findings. Firstly, the difference between the first heating to above $T > T_g$ and subsequent thermal cycling of the highly deformed foils now corresponds to a densification of about 0.4% of volume per atom. This indicates that heavy deformation (thickness reduction of 90–97%) has resulted in the generation of free-volume to a level double that of the same glass in the as-quenched state. This result is consistent with the generation of free-volume during heterogeneous deformation of metallic glasses known to occur in shear bands [31] as also previously reported by dilatometric methods [4]. Secondly, the higher free-volume content in the deformed foils results in faster relaxation kinetics now detectable above 400 K. The total free-volume generation during deformation is likely more than what is detected here as some free-volume may precipitate into large holes [32,33] that do not significantly modify the mean interatomic distance. Perhaps most significantly, the relaxed states of

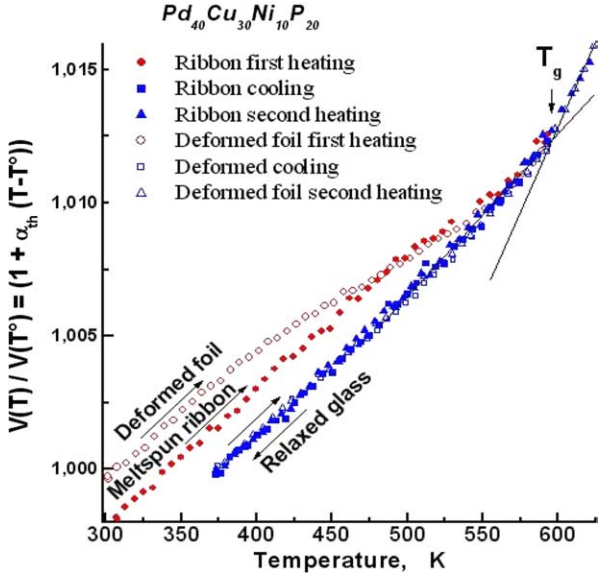

Fig. 8. Reduced volume per atom of Eq. (2) showing relaxation of both as-quenched ribbon and heavily deformed foils of the glass towards the same relaxed glassy state attained near T_g; slope (thermal expansion coefficient) change at T_g is clearly visible.

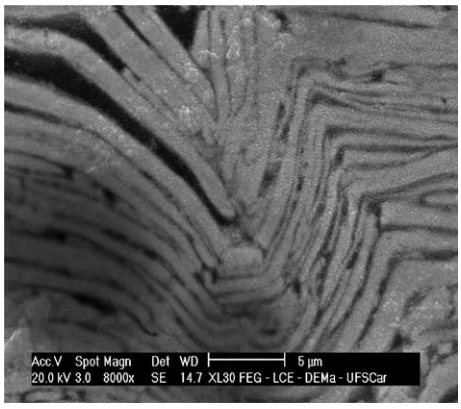

Fig. 9. SEM image of ribbon stacks after "gentle" milling showing a thickness reduction from initial about 30 μm to about 1–3 μm.

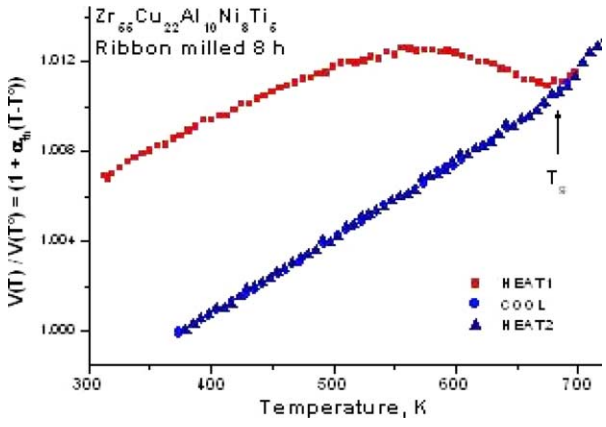

Fig. 10. Reduced volume per atom of Eq. (4) showing relaxation of heavily deformed foils of the ZrCuAlNiTi glass near T_g.

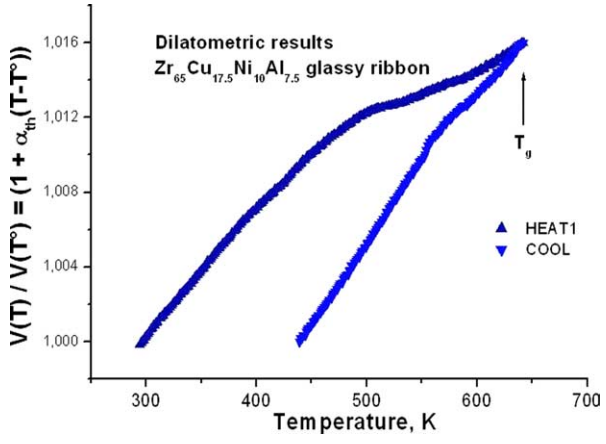

Fig. 11. Length change (dilatation) of a glassy $Zr_{65}Cu_{17.5}Ni_{10}Al_{7.5}$ melt-spun ribbon showing densification towards the relaxed glassy state attained near T_g [34].

the material after rapid quenching and after heavy deformation exhibit exactly the same volume with near constant thermal expansion and a break in α_{th} at T_g. Comparing the shapes of the plots of Figs. 5 and 8 with the most well established dilatometric data for easy glass-forming alloys as for example reproduced in Fig. 7, one notes that both follow the same thermal behaviour. We obtained similarly shaped data for metal–metal type glasses (Fig. 10) that also compare well with dilatometric curves (Fig. 11 reproduced from [34]).

4. Discussion

The present in situ diffraction experiments thus indicate that the average interatomic volume in these metallic glasses as deduced from X-ray diffraction scales with the macroscopic specimen dimensions (length change) as measured with dilatometry and that Eq. (4) can be used to follow variations of free-volume content.

This is in contrast to the creation of vacant sites on a crystal lattice (or transfer of atoms from those sites to the crystal surface, see Fig. 12) which leads to an increase in the crystal dimension but does not significantly change the average interatomic or interplanar distances as determined by the application of the Bragg law to the lattice's X-ray diffraction lines.

In 1960, at the same time as the first metallic glasses were discovered, Simmons and Balluffi [35] devised experiments allowing precise determination of equilibrium lattice vacancies in crystals by simultaneously measuring the length change $\Delta L/L$ (by dilatometry) and lattice parameter change $\Delta a/a$ (by X-ray diffraction). Their experiments which contributed to the quantitative understanding of point defects in solid-state physics [36] were based on the following simple equation for the vacant fraction of lattice sites C_v as a function of temperature T:

$$C_v(T) = 3\left\{\frac{(\Delta L(T)}{L_0} - \frac{\Delta a(T)}{a_0}\right\}, \tag{5}$$

where $\Delta a(T)/a_0 = \alpha_{th}(T)*(T - T_0)/a_0$, L_0 and a_0 are the crystal length and lattice parameter at a reference temperature T_0, and $\alpha_{th}(T)$ the linear coefficient of thermal expansion, itself weakly temperature-dependent [37]. Their experiments showed that C_v is nearly zero in a relaxed crystal at low temperatures but increases to tens and hundreds of ppm (less than 10^{-3}) as thermal vacancies are generated at high temperatures. To recapitulate, Simmons and Balluffi used the lattice parameter change $\Delta a(T)/a_0$ measured by X-ray diffraction to remove the part of the length-change due to the thermal expansion of the lattice. What remains of $\Delta L(T)/L_0$ then yields the increase in vacant lattice sites.

If as in crystals, quenched-in free-volume in the glassy state took the form of atomic size holes such as in Fig. 13(b), a combination of dilatation and X-ray diffraction measurements would be needed to determine V_f as for vacancies in crystals.

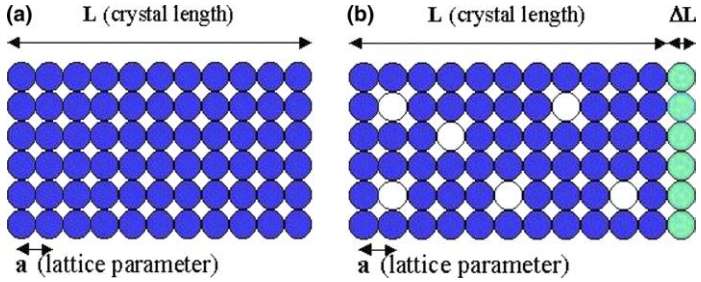

Fig. 12. (a) Crystal lattice with no vacancies. (b) Vacancies introduced in the crystal.

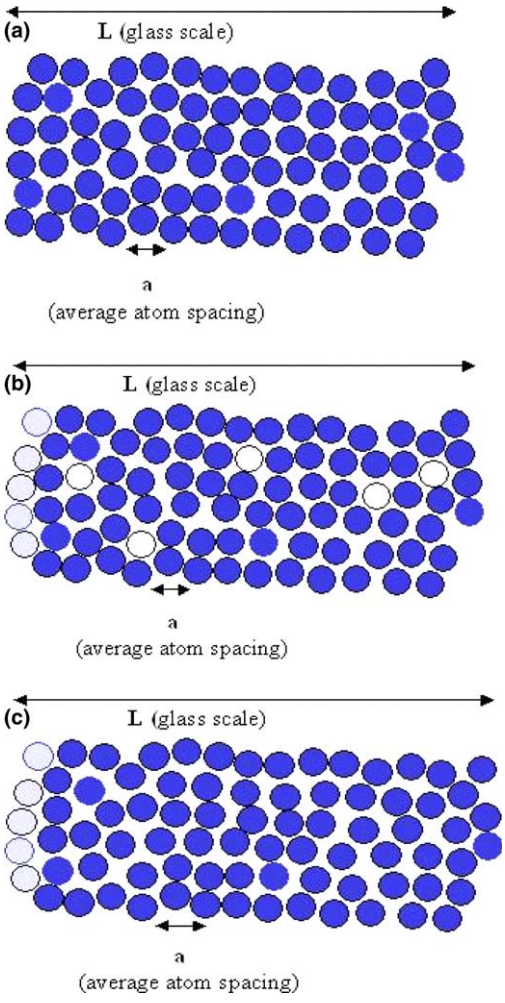

Fig. 13. (a) Two-dimensional scheme of monatomic glass; (b) glass with atomic size holes; (c) glass with holes dispersed randomly throughout the volume.

On the other hand, if as computer simulation predicted [38,39], atomic size holes or vacancies in a glass are unstable and the quenched-in free volume in liquids and glasses is randomly distributed (Fig. 13(c)), Eq. (5) of Simmoms and Balluffi would not apply, $\Delta V(T)/V_0$ would be equal to $3\Delta L(T)/L_0$ and the mean atomic volume and the sample dimensions would evolve together with temperature as observed here.

The fact that the average interatomic volume in metallic glasses as deduced from X-ray diffraction scales with the macroscopic specimen dimensions (length change) as measured with dilatometry (comparison of Figs. 6 and 8) would thus correspond to $\Delta L(T)/L_0 = \Delta a(T)/a_0$ in the Simmons and Balluffi equation.

This finding is consistent with computer simulation predicting [38] that atomic size holes or vacancies in a glass are unstable and free volume in liquids and glasses is randomly distributed as in Fig. 13(c).

Similar results have been obtained for Zr-based metal–metal glasses [13] and a wide variety of other quenched and deformed glasses. For example, the method has been applied successfully to oxide glasses such as window glass as recently demonstrated for pyrex (see Fig. 14 reproduced from [40]).

These measurements also allow studies of the kinetics of relaxation and the thermal annealing-out of the free-volume. Metallic glasses are known to be of the "fragile" type [41,42] corresponding to an activation energy E for viscous and diffusive flow that is temperature dependent with E increasing with T (a non-Arrhenius behaviour) [43] as expected for example from relation (1) or a Vogel–Fultcher–Tamman viscosity relation

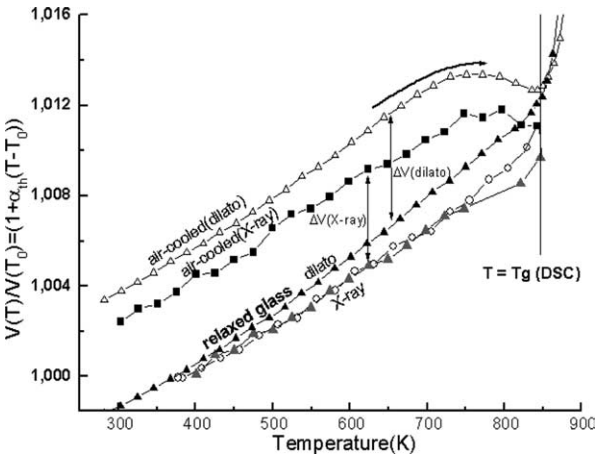

Fig. 14. Comparison of the volume thermal expansion of air-cooled borosilicate pyrex glasses obtained by conventional dilatometry and X-ray diffraction [40].

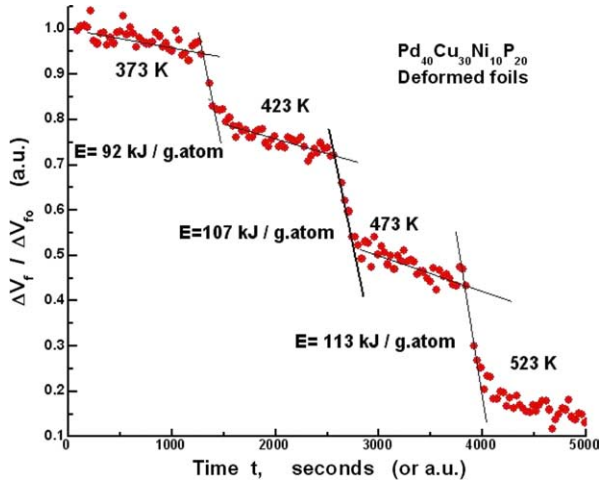

Fig. 15. Change-of-slope method of Eq. (7) applied during in situ isothermal diffraction experiments: isothermal relaxation kinetics of excess free volume in heavily deformed glassy foil of Figs. 8 and 9 when the temperature is abruptly changed at time t^* from T_i to T_{i+1}. The activation energy E can be obtained from the slope change $dV_f(T_1, t^*)/dt$ to $dV_f(T_2, t^*)/dt$ according to Eq. (7).

[41,42]. However, the kinetics of isothermal relaxation [40] can be written as:

$$\frac{dV_f(T,t)}{dt} = -F(V_f)K_0 e^{\frac{-E}{RT}}, \tag{6}$$

where $F(V_f)$ is any continuous function of V_f and K_0 is the pre-exponential of a rate constant with activation energy E and R is the gas constant [44]. This type of rate equation has been previously applied to isothermal relaxation of viscosity, resistivity, elastic constants and enthalpy in quenched metallic glasses [25,30,45]. It can be shown [40] from Eq. (6) that if during isothermal relaxation the temperature is abruptly changed at time t^* from T_1 to T_2, the activation energy E can be obtained from the slope change dV_f $(T_1, t^*)/dt$ to dV_f $(T_2, t^*)/dt$ according to:

$$\ln \frac{dV_f(T_1,t^*)/dt}{dV_f(T_2,t^*)/dt} = \frac{E}{R}\left\{\frac{1}{T_1} - \frac{1}{T_2}\right\}. \tag{7}$$

Fig. 15 shows the result of such experiments performed during in the beam annealing out of free volume in foils of glassy $Pd_{40}Cu_{30}Ni_{10}P_{20}$ obtained after severe deformation. These isothermal relaxation curves may be compared to similar isothermal densification curves reported in [46] using dilatometric techniques. The method yields a temperature-dependent E for structural relaxation leading to free-volume annihilation below T_g. E increases from 92 kJ/g.atom near 400 K to 114 kJ/g.atom near 500 K.

In conclusion, thermal expansion coefficient α_{th} of glassy $Pd_{40}Cu_{30}Ni_{10}P_{20}$ was measured during heating cycles by in situ X-ray diffraction in transmission and the results are the same as those of dilatometry. This indicated that contrary to the case of vacancies in crystals, free volume in glasses can be directly measured by diffraction methods. Both quenched-in and deformation-induced free-volume ΔV_f were measured and found to fully relax during heating up to T_g at which temperature all thermo-mechanical history of the metallic glass was erased. The glass transition T_g appears clearly as a break in the value of α_{th} as the glass transforms to a supercooled liquid state during heating. The change-of-slope method was applied to the kinetics of relaxation to derive the activation energy for the free-volume annihilation process.

Acknowledgements

This work was performed in the framework of the EU Network on bulk metallic glass composites (MRTN-CT-2003-504692 <Ductile BMG Composites>) coordinated by A.R. Yavari, Tohoku University's International Frontier Centre for Advanced Materials (IFCAM) and the long-term project entitled: "Study of the glass transition in bulk metallic glasses by diffraction methods" at the European synchrotron (ESRF). Thanks are also due to K. Hajlaoui for his contribution to the experiments.

References

[1] Cohen MH, Turnbull D. J Chem Phys 1959;31:1164.
[2] Klement W, Willens RH, Duwez P. Nature 1960;187:869.
[3] Greer AL. Science 1995;267:1947.
[4] Chen HS. J Appl Phys 1978;49:3289.
[5] Kui HW, Greer AL, Turnbull D. Appl Phys Lett 1984;45:615.
[6] Inoue A. Acta Mater 2000;48:279.
[7] Johnson WL. MRS Bull October 1999; 42–56.
[8] Inoue A, Shen B, Koshiba H, Kato H, Yavari AR. Nature Mater 2003;2:661.
[9] Spaepen F. Acta Metall 1977;25:407.
[10] Argon A. Acta Metall 1979;27:47.
[11] Steif PS, Spaepen F, Hutchinson JW. Acta Metall 1982;30:447.
[12] Chen HS, Krause JT, Sigety EA. J Non-Cryst Solids 1973/74;13:321.
[13] Yavari AR, Tonegaru M, Lupu N, Inoue A, Matsubara E, Vaughan G, et al. J Mater Res Symp Proc 2004;806:203.
[14] Yavari AR, Nikolov N, Nishiyama N, Zhang T, Inoue A, Uriarte JL, Heunen G. Mater Sci Eng A 2004;375–377:709.
[15] Yavari AR, Inoue A, Botta WJ, Kvick A. Scripta Mater 2001;44:1239.
[16] Yavari AR, LeMoulec A, Inoue A, Vaughan G, Kvick A·A. Annal Chimie Sci des Matér 2002;27:107.
[17] Cromer DT, Mann JB. J Chem Phys 1967;47:1892.
[18] Waseda Y. The structure of non-crystalline materials. McGraw-Hill Inc; 1980.
[19] Ibers JA, Hamilton WC, editors, International tables for X-ray Crystallography, vol. IV. Birmingham (present distributor Kluwer Academic Publishers, Dordrecht): Kynoch Press. p. 148–50.
[20] Cromer DT, Liberman DL. J Chem Phys 1970;53:1891.
[21] Waseda Y, Egami T. J Mater Sci 1979;14:1249.
[22] Chen HS, Aust KT, Waseda Y. J Mater Sci Lett 1983;2:153.

[23] Inoue A, Negishi T, Kimura HM, Zhang T, Yavari AR. Mater Trans JIM 1998;39:318.
[24] Mattern N, Küln U, Hermann H, Roth S, Vinzelberg H, Eckert. J Mater Sci Eng 2004;375–377:351.
[25] Van Den Buekel A, Sietsma J. Acta Metall Mater 1990;38:383.
[26] Turnbull D. In: Hughel TJ, editor. Liquids: structure, properties, solid interactions. Amsterdam: Elsevier; 1965. p. 6–24.
[27] Guinier A. Théories et Techniques de la Radio-christalographie. Dunod; 1964.
[28] Yavari AR. Acta Metall 1988;36:1863.
[29] Nishiyama N, Horino M, Inoue A. Mater Trans JIM 2000;41:1432.
[30] Taub A, Spaepen F. Acta Metall 1980;28:1781.
[31] Donovan PE, Stobbs WM. Acta Metall 1981;29:1419.
[32] Li J, Spaepen F, Hufnagel TC. Phil Mag 2002;A82:2623.
[33] Wright WJ, Hufnagel TC, Nix WD. J Appl Phys 2003;93:1432.
[34] Schermeyer D, Neuhäuser H. Mater Sci Eng 1997;A226–228: 846.
[35] Simmons R, Balluffi R. Phys Rev 1960;117:52.
[36] Seeger A, Schumacher D. In: Cotterill RMJ, Doyama M, Jackson JJ, Meshii M, editors. Lattice defects in quenched metals. Academic Press; 1965. p. 15–75.
[37] Vinet P, Smith JR, Ferrante J, Rose JH. Phys Rev B 1987;35:1945.
[38] Bennett CH, Chaudhari P, Moruzzi V, Steinhardt P. Phil Mag A 1979;40:485.
[39] Faupel F, Frank W, Macht M, Mehrer P, Naundorf H, Rätzke V, et al. Rev Mod Phys 2003;75:237.
[40] Ota K, Botta WJ, Vaughan G, Yavari AR. J Alloy Compd 2004 [in press].
[41] Angell CA. Science 1995;267:1925.
[42] Busch R, Masuhr A, Johnson WL. Mater Sci Eng A 2001;304:97.
[43] Bobrov OP, Khonik VA, Laptev SN. Scripta Mater 2004;50:337.
[44] Damask AC, Dienes GJ. Point defects in metals. Gordon and Breach. p. 146–49.
[45] Huizer E, Mulder AL, Van den Beukel A. Acta Metall 1986;34:493.
[46] Russew K, Sommer F. J Non-Cryst Solids 2003;319:289.